ChemComm

Single-component frameworks for heterogeneous catalytic hydrolysis of organophosphorous compounds in pure water

Journal:	*ChemComm*
Manuscript ID	CC-COM-03-2019-002236.R1
Article Type:	Communication

ChemComm

COMMUNICATION

Single-component frameworks for heterogeneous catalytic hydrolysis of organophosphorous compounds in pure water

Sergio J. Garibay,[a] Omar K. Farha*[b] and Jared B. DeCoste *[a]

Received 00th January 20xx,
Accepted 00th January 20xx

DOI: 10.1039/x0xx00000x

www.rsc.org/

Amine modified Zr_6-based metal-organic frameworks (MOFs) were synthesized through solvent-assisted linker incorporation (SALI) and utilized as single-component heterogeneous catalysts for the hydrolysis of organophosphorous compounds under solely aqueous conditions at room temperature. These materials display unprecidentedly fast catalytic hydrolysis for dimethyl *p*-nitrophenyl phosphate (DMNP) and nerve agent VX without the use of a buffered solution.

Although the use of chemical warfare agents (CWAs) have been outlawed by the Chemical Weapons Convention (CWC),[1] recent geopolitical events have prompted renewed efforts in developing protective methods for their efficient destruction.[2,3] Nerve agents, CWAs containing phosphonate groups, are extremely toxic to the nervous system. These organophosphonate compounds covalently bind to an enzyme, acetylcholinesterase (AChE), responsible for the catalytic breakdown of acetylcholine which functions as a neurotransmitter to muscles and organs.[4] Subsequent build-up of acetylcholine prevents contraction of muscles and organs vital to respiration resulting in death by asphyxiation or cardiac arrest. While nerve agents can be rendered ineffective by enzymes, through catalytic hydrolysis and cleavage of the P-X (X = F, CN, or S) bond, their use is limited by insufficient stability under practical conditions.[5] Consequently, stable materials capable of catalytic hydrolysis of organophosphorous compounds, such as zeolites, polyoxometalates, metal oxides, and recently metal-organic frameworks (MOFs), have been applied to the destruction of CWAs.[6]

MOFs are crystalline porous materials comprised of organic struts which link to metal clusters, *i.e.* secondary building units (SBUs) periodically forming hybrid networks. Utilization of Zr_6-based SBUs have resulted in chemically robust MOFs amenable to functionalization, node and strut alteration, which enables their use in realistic and catalytic conditions.[7] The Zr_6 SBU is ideally 12-connected, *i.e.* 12 carboxylic acids bound to the SBU, but 10, 8, 6 or 4-connected can be obtained depending on reaction conditions and the multi-topic organic strut employed in MOF synthesis.[8] MOFs containing SBUs with a connectivity less than 12 possess so-called "missing-linkers" sites that are often occupied by modulators, *i.e.* mono carboxylic acids, employed during construction of the MOF.[9] The use of modulators during MOF synthesis has been shown to regulate MOF crystallinity, particle size and affect the amount of missing-linker or missing-node defects.[10, 11] Due to the chemical robustness of the Zr_6 SBU, the modulators can be readily removed to give $Zr(OH)(OH_2)$ sites through thermal or acidic activating conditions without structural damage to the framework. These deficient sites have been exploited as handles for modification such as solvent-assisted linker incorporation (SALI),[12] and solvothermal- or atomic layer-deposition in MOFs (SIM or AIM),[12, 13] which enables the inclusion of catalytically active species.

It has been recently shown that these deficient "missing-linker" sites facilitate rapid hydrolysis of organophosphorous compounds.[14, 15] However, alkaline buffer conditions are often required for fast hydrolysis rates.[16] Indeed, under neutral aqueous conditions many Zr-MOFs do not catalytically hydrolyze organophosphorous compounds.[17] This is likely due to the function of the buffer to aid in proton transfer as well as repopulate the hydroxyl groups on the SBU.[15] While many have explored the development of Zr-MOF composites, they often lead to slower hydrolysis rates due to the inhomogeneity of the MOF filler particles with hydrophobic matrix components,[18] which are often needed in excess due to leaching of amine containing components.[19] Consequently, MOFs alone must be capable of facilitating conditions that enable fast nerve agent catalytic hydrolysis in order for realistic use in the field. Herein, we report the use of SALI to develop amine functionalized Zr-

[a] *Combat Capabilities Development Command Chemical and Biological Center, 5183 Blackhawk Road, Aberdeen Proving Ground, Maryland 21010, USA.*
[b] *Department of Chemistry, International Institute of Nanotechnology, Northwestern University, 2145 Sheridan Road, Evanston, Illinois 60208, USA.*
Electronic Supplementary Information (ESI) available: [MOF modification, characterization and hydrolysis procedures]. See DOI: 10.1039/x0xx00000x

MOFs that act as single-component catalysts for degradation of organophosphorous compounds under solely aqueous conditions (Scheme 1).

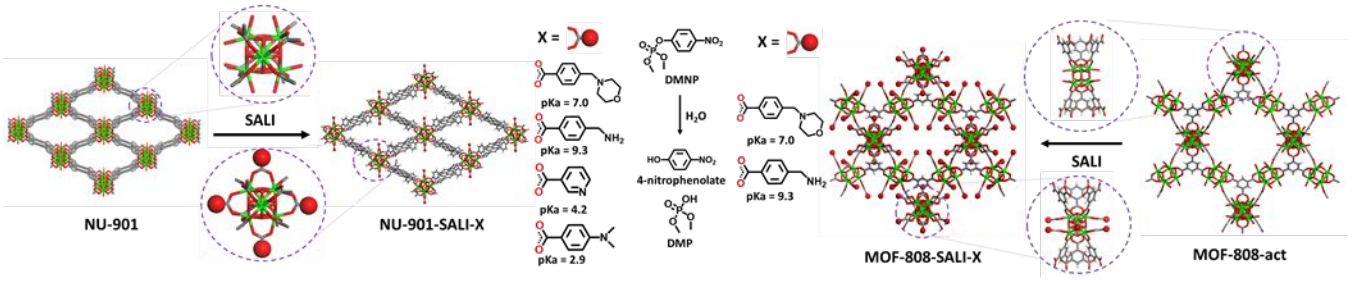

Scheme 1. Solvent-assisted linker incorporation (SALI) of amine functionalized modulators within NU-901 and MOF-808 utilized for the hydrolysis of organophosphorous compounds in pure water. pKa values were calculated through Chemicalize (ChemAxon).

NU-901, is comprised of 8-connected Zr_6 SBU nodes (4 missing-linkers) and 1,3,6,8-tetrakis-(*p*-benzoate)-pyrene (H_4TBAPy) linkers that form microporous diamond-shaped channels with **scu** topology. Recently, we demonstrated enhanced CO_2 adsorption through incorporation of amine-functionalized mono carboxylate modulators within the Zr_6 SBUs of NU-901.[20] Given that the Lewis-basic amine moieties were shown to significantly alter the pore surface's enthalpy of adsorption for CO_2, it was hypothesized that amine functionalities adjacent to the SBU would facilitate the hydrolysis of organophosphorous compounds. Amine functionalities on the organic struts of Zr-based MOFs have been previously shown to significantly enhance the hydrolysis of organophosphorous compounds under N-ethylmorpholine (NEM) buffer conditions.[21] However, the pKa of aromatic amines (~1) are insufficient to promote base hydrolysis and the vast majority of MOFs are rarely active under solely aqueous conditions. Here we examine a variety of amine functionalized NU-901 materials for the hydrolysis of the G-agent simulant dimethyl-4-nitrophenyl phosphate (DMNP) in pure water.

We examined these SALI functionalized MOFs in the hydrolysis of DMNP in water with 4 mol% catalyst loading through ^{31}P NMR. A control experiment with HCl-activated NU-901 did not show any significant conversion to the hydrolysis product dimethyl phosphate anion (DMP) (<5 % conversion after 18 h, Fig. S19). Only NU-901-SALI-[BA-N$(CH_3)_2]_1$ and NU-901-SALI-$[nico]_2$ (BA = benzoic acid, nico = nicotinic acid) displayed any activity in DMNP hydrolysis (Table 1, Fig. S20). However, given that these MOFs displayed modest activity (~30 % conversion after 18 h), we set out to incorporate other amine functionalities possessing higher basicity that would enable faster hydrolysis.

As stated above, NEM buffer has been used to act as a base and fast hydrolysis of organophosphorous compounds with Zr-based MOFs, consequently, we attempted heterogenization of this buffer through the use of 4-(morpholinomethyl)benzoic acid (BA-morph). In our previous SALI functionalization attempts with NU-901, incorporation of amine containing benzoic acid modulators were limited by the reduced acidity of the carboxylic acid. However, SALI with ~16 equivalents of BA-morph resulted in nearly full functionalization (3.5 modulators per Zr_6 SBU) of NU-901. This result suggests that BA-morph has sufficient acidity to readily bind to the missing-linker sites within NU-901. The use of 9 mol% of NU-901-SALI-$[BA\text{-}morph]_{3.5}$ displayed hydrolysis of DMNP (~30% conversion after 18 h, Table 1, Fig. S22). However, the MOF may not contain sufficient missing-linker sites to facilitate hydrolysis due to 3.5 of the 4 active sites per SBU being occupied by BA-morph.

To examine if hydrolysis is enhanced by increasing the amount of missing-linker sites, we decreased the incorporation of BA-morph to 2 per SBU. Interestingly, a reduction in DMNP hydrolysis was observed when NU-901-SALI-$[BA\text{-}morph]_2$, containing two missing-linker sites, was utilized under identical catalytic conditions (~30% vs 10% conversion after 18h, Table 1, Figs. S22-23). This goes against the established observation of enhanced DMNP hydrolysis with more missing-linker sites under NEM buffered conditions.[22] This result suggests that the degree of basicity and the amount of the modulator within the single-component MOFs are integral for hydrolysis to occur under solely aqueous conditions.

Table 1. Surface area, # of moieties incorporated, catalyst loading of amine modified MOFs and their activity towards hydrolysis of DMNP and VX.

MOF	Surface area (m^2/g)[a]	Moieties Incorp.[b]	Zr_6 SBU/ DMNP[c]	DMNP /free Zr site	$t_{½}$
NU-901-act[d]	2276	0	4 %	6.3	> 18 h
NU-901-[BA-N$(CH_3)_2$]	2029	1	4 %	8.3	> 18 h
NU-901-SALI-$[nico]_2$	1770	2	4 %	12.5	> 18 h
			15 %	3.3	> 18 h
NU-901-SALI-$[BA\text{-}morph]_{3.5}$	1313	3.5	9 %	22.1	> 18 h
			15 %	13.3	15 min
NU-901-SALI-$[BA\text{-}morph]_2$	1362	2	9 %	5.5	> 18 h
NU-901-SALI-$[BA\text{-}CH_2NH_2]_2$	1203	2	4 %	12.5	90 min
			9 %	5.5	20 min
			15 %	3.3	5 min
MOF-808-P	1387	4[e]	9 %	5.5	180 min
MOF-808-act[d]	1734	3[f]	9 %	3.6	300 min
MOF-808-SALI-$[BA\text{-}morph]_3$	574	3	9 %	3.6	11 min
			15 %	2.2	9 min
MOF-808-SALI-$[BA\text{-}CH_2NH_2]$ $[BA\text{-}CH_2\text{-}NH_3^+]$	773	2	9 %	5.5	180 min
			15 %	3.3	53 min
MOF-808-act[d] (VX)	1734	3	12 %	2.8	5 min[g]
MOF-808-SALI-$[BA\text{-}morph]_3$ (VX)	574	3	12 %	2.8	< 1 min[g]
MOF-808-SALI-$[BA\text{-}CH_2NH_2]$ $[BA\text{-}CH_2\text{-}NH_3^+]$ (VX)	773	2	12%	2.2	< 1 min[g]

[a] BET. [b] Per node, based on ^{1}H NMR of digested samples. [c] catalyst loading. [d] HCl-activated. [e] incorporated through *de novo* synthesis. [f] Formic acid generated by DMF decomposition. [g] estimated by number of half-lives reached at first point

In order to test this hypothesis and enhance conversion, we explored the effect of increasing the catalyst loading on the hydrolysis of DMNP. While the use of NU-901-SALI-[BA-nico]$_2$ at 15 mol% catalyst loading resulted in a slight enhancement in hydrolysis (~30% conversion within 2 h vs 18 h at 4 mol%, Table 1, Fig. S21), the use of NU-901-SALI-[BA-morph]$_{3.5}$ under the same loading could not be clearly monitored by ^{31}P NMR as the amount of MOF masked the signal (Table 1, Fig. S24). This led us to re-examine hydrolysis by filtering the MOF at various time points. After 10 and 20 min the use of NU-901-SALI-[BA-morph]$_{3.5}$ at 15 mol% loading resulted in 40 and 75% conversion, respectively.

Given that increased modulator incorporation and fewer missing-linker sites within NU-901-SALI-[BA-morph]$_{3.5}$ enhances DMNP hydrolysis, the role and exact placement of the modulator throughout the reaction was examined. Spent NU-901-SALI-[BA-nico]$_2$ and NU-901-SALI-[BA-morph]$_{3.5}$ of the aforementioned 15 mol% hydrolysis reactions were recovered and washed with dimethylformamide and methanol. The ^{1}H NMR spectra of the digested recovered materials revealed that some within NU-901-SALI-[BA-nico]$_2$ (0.5 per node out of 2 per node) and all of the modulators within NU-901-SALI-[BA-morph]$_{3.5}$ were lost after hydrolysis (Figs. S2, S5). This suggests that the modulators dissociate from the Zr_6 SBU during the reaction, creating additional sites for hydrolysis to occur. The modulators are replaced by DMP on the SBU as indicated by the emergence of a new chemical shift (~ 3.5 ppm) in the ^{1}H NMR spectra (Figs. S2, S5). Hill and co-workers reported that DMP can poison catalytic sites within Zr-containing polyoxometalates inhibiting DMNP hydrolysis.[16] Moreover, Lang and co-workers recently reported that modulators within UiO-66 dissociate under aqueous organophosphate solutions, which leads to additional missing-linker defects and consequently faster hydrolysis of DMNP.[23] However, control DMNP hydrolysis experiments with modulators alone or their *in situ* combinations with HCl activated NU-901 did not result in significant hydrolysis, presumably due to water insolubility and zwitterionic inhibition (Figs. S28, S29). While the possibility of dissociated modulators participating in DMNP hydrolysis cannot be ruled out, the control experiments suggest that modulators must be covalently bound to the Zr_6 SBU in order to facilitate fast hydrolysis.

Since the preceding functionalized MOFs resulted in modest hydrolysis rates of DMNP, the use of 4-(aminomethyl)benzoic acid (BA-CH_2NH_2), which possesses higher basicity (pK_a = 9.33) was explored.[24] Functionalization of NU-901 with this modulator resulted in two benzylamine moieties per Zr_6 node as indicated by ^{1}H NMR (Fig. S6). Faster DMNP hydrolysis was observed with 4 mol% catalyst loading of NU-901-SALI-[BA-CH_2NH_2]$_2$ under aqueous conditions ($t_{½}$ > 90 min, Table 1, Figure S25). Increasing the catalyst loading to 9 or 15 mol% greatly accelerated hydrolysis ($t_{½}$ = 20 and 5 min, respectively, Table 1, Fig. S26, S27). Interestingly, the DMNP hydrolysis reaction profiles in all catalyst loadings exhibit plateaus around 15 to 30 minutes after fast initial conversion. It is likely that this change in hydrolysis could be attributed to the DMP partially displacing the modulators within the MOF (Scheme S1). We have previously reported that phosphate groups bind more readily to missing linker sites than carboxylate groups within Zr_6 SBUs.[25] In another study, we observed the dissociation of carboxylic acids bound within the 8-connected Zr_6 SBU of NU-1000 after prolonged utilization in olefin epoxidation with aqueous H_2O_2.[26] The dissociation of these carboxylic acids leads to a gradual decrease in the catalytic activity which can be renewed upon restoration of the initial number of carboxylic acids by post-synthetic treatment.

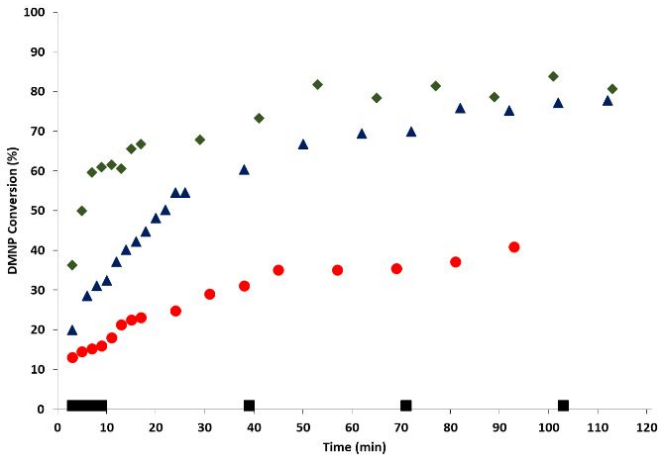

Figure 1. DMNP hydrolysis with NU-901-act (black squares), NU-901-SALI-[BA-CH_2NH_2]$_2$ at 4 mol% (red circles), 9 mol% (blue triangles), and 15 mol% (green diamonds) catalyst loading.

As previously mentioned, Zr_6-based MOFs can have various topologies depending on the degree of missing-linker sites and the type of carboxylic acid organic linker. Consequently, we sought to generalize our single-component strategy towards hydrolysis of organophosphorous compounds with different Zr_6-based MOFs. MOF-808 is comprised of 6-connected Zr_6 SBUs with 1,3,5-benzenetricarboxylic acid (BTC) linkers with a formula of $Zr_6O_4(OH)_4(BTC)_2(A)_6$ (A = mono-carboxylic modulator) and **spn** topology.[27] Surprisingly, as synthesized MOF-808-P, containing 4 propanoic acid modulators, displayed DMNP hydrolysis in aqueous non-buffered conditions ($t_{½}$ = 180 min at 9 mol% loading, Table 1, Fig. S30). This suggests that the propanoic acid modulators are facilitating enhanced DMNP hydrolysis. This results mirrors Hill and co-workers observation that acetate buffer significantly accelerated the hydrolysis of DMNP with Zr-containing polyoxometalates.[16] HCl-activated MOF-808 also displayed significant DMNP hydrolysis ($t_{½}$ = 300 min at 9 mol% loading, Table 1, Fig. S31). The observed activity is hypothesized to be a consequence of DMF decomposition byproducts (formic acid and dimethylammonium chloride) binding within the SBUs of MOF-808 during HCl activation.[28] Indeed, ^{1}H NMR of the digested MOF-808-act displays peaks associated with 3 formic acid and dimethylammonium byproducts per Zr_6 SBU (Fig. S7).

Nonetheless, hydrolysis was further enhanced utilizing the single-component approach with amine modification of MOF-808. Through the use of SALI, 2 BA-CH_2NH_2 and 3 BA-morph amine containing modulators per SBU were incorporated into MOF-808, as evidenced by ^{1}H NMR (Fig. S8, S9). Interestingly,

the NMR spectrum of MOF-808 modified with BA-CH_2NH_2 contains four aromatic stretches and two sets of methanediyl groups which we attribute to amine protonation within approximately half of the incorporated modulators (Fig. S9). Incorporation of the modulators significantly reduces surface area (Table 1) and pore size (13 vs 16 Å, Fig. S14) while altering the relative peak intensities of the (311) and (222) planes in the PXRD pattern (Fig. S16). MOF-808-SALI-[BA-CH_2NH_2][BA-CH_2-NH_3^+] displayed slower hydrolysis than MOF-808-SALI-[BA-morph]$_3$ at 9 or 15 mol% loading (Table 1). This relative decrease in rates of MOF hydrolysis may be a consequence of lower amounts of incorporated modulators with free amine moieties or the protonated amine creating a more acidic microenvironment. Similar to the NU-901 materials, both amine-functionalized MOF-808 materials lost a significant number of modulators (1 remaining per node for each material) (Fig. S10, S11). The observed hydrolysis with SALI modified MOF-808 materials are not due to decomposition, as the spent materials display intact PXRD patterns (Fig S17, S18) and filtration of MOF-808-SALI-[BA-morph]$_3$ after 10 min inhibits further conversion (Fig. S36). Moreover, the modulators do not leach after prolonged aqueous exposure (Fig. S37, S38). Given that some modulators remain after reaction, these control experiments further suggest that hydrolysis derives from the traditional missing-linker mechanism being co-catalyzed by the neighboring basic amine functional groups (Scheme S1).

While DMNP is an adequate simulant, our successful single-component MOFs results prompted examination of an actual nerve agent. Under solely aqueous conditions, both amine functionalized MOFs facilitate near instantaneous and full hydrolysis of VX (Table 1, Figs. S39, S40). The ^{31}P NMR spectra indicate selective formation of non-toxic EMPA hydrolysis product with trace (<1%) amounts of EA-2192 originating from impurities within the VX sample (Fig S41). We note that hydrolysis of VX under non-buffered conditions with MOF-808 has been previously observed. Activity was shown to be attributed to the N-propyl amine moiety within VX self-buffering itself with the Zr_6 SBU.[17] However, under similar conditions MOF-808-act displays slower hydrolysis of VX than our single-component MOFs (Table 1, Fig. S42).

In conclusion, we have successfully shown that modification of MOFs with amine-containing mono-carboxylic acid modulators enable catalytic hydrolysis of organophosphorous compounds without the need of buffer solutions. The single-component strategy was shown to be applicable for a variety of Zr_6-based MOFs containing missing-linker sites. While the amine modulators enabled hydrolysis, they are ultimately displaced by the dimethyl phosphate acid by-product resulting in eventual catalytic poisoning of the Zr sites. Further efforts understanding the mechanistic pathway and SBU environment of these MOFs through *operando* spectroscopic techniques in solution and solid-state will be explored. Our impressive single-component approach is a step closer toward implementation of protective MOF composites within filter masks or clothing for effective destruction of CWAs.

Conflicts of interest

There are no conflicts to declare.

Notes and references

1. U. Nations, *Convention on the Prohibition of the Development, Production and Stockpiling of Bacteriological (Biological) and Toxin Weapons and on their Destruction*, 1972.
2. M. Enserink, *Science*, 2013, **341**, 1050-1051.
3. Progress in the Elimination of the Syrian Chemical Weapons Programme, https://www.Opcw.Org/Media-Centre/Featured-Topics/Syria-and-Opcw, accessed Feb. 18, 2018).
4. A. Watson, D. Opresko, R. A. Young, V. Hauschild, J. King, K. Bakshi and R. C. Gupta, in *Handbook of Toxicology of Chemical Warfare Agents (Second Edition)*, Academic Press, Boston, 2015, pp. 87-109.
5. P. Li, Q. Chen, T. C. Wang, N. A. Vermeulen, B. L. Mehdi, A. Dohnalkova, N. D. Browning, D. Shen, R. Anderson, D. A. Gómez-Gualdrón, F. M. Cetin, J. Jagiello, A. M. Asiri, J. F. Stoddart and O. K. Farha, *Chem*, 2018, **4**, 1022-1034.
6. B. M. Smith, *Chem. Soc. Rev.*, 2008, **37**, 470-478.
7. M. Kim and S. M. Cohen, *CrystEngComm*, 2012, **14**, 4096-4104.
8. Z. Chen, S. L. Hanna, L. R. Redfern, D. Alezi, T. Islamoglu and O. K. Farha, *Coordin. Chem. Rev.*, 2019, **386**, 32-49.
9. J. E. Mondloch, W. Bury, D. Fairen-Jimenez, S. Kwon, E. J. DeMarco, M. H. Weston, A. A. Sarjeant, S. T. Nguyen, P. C. Stair, R. Q. Snurr, O. K. Farha and J. T. Hupp, *J. Am. Chem. Soc.*, 2013, **135**, 10294-10297.
10. A. Schaate, P. Roy, A. Godt, J. Lippke, F. Waltz, M. Wiebcke and P. Behrens, *Chem. Eur. J.*, 2011, **17**, 6643-6651.
11. F. Vermoortele, B. Bueken, G. l. Le Bars, B. Van de Voorde, M. Vandichel, K. Houthoofd, A. Vimont, M. Daturi, M. Waroquier and V. Van Speybroeck, *J. Am. Chem. Soc.*, 2013, **135**, 11465-11468.
12. T. Islamoglu, S. Goswami, Z. Li, A. J. Howarth, O. K. Farha and J. T. Hupp, *Acc. Chem. Res.*, 2017, **50**, 805-813.
13. Z. Li, A. W. Peters, V. Bernales, M. A. Ortuño, N. M. Schweitzer, M. R. DeStefano, L. C. Gallington, A. E. Platero-Prats, K. W. Chapman, C. J. Cramer, L. Gagliardi, J. T. Hupp and O. K. Farha, *ACS Central Science*, 2017, **3**, 31-38.
14. J. E. Mondloch, M. J. Katz, W. C. Isley Iii, P. Ghosh, P. Liao, W. Bury, G. W. Wagner, M. G. Hall, J. B. DeCoste, G. W. Peterson, R. Q. Snurr, C. J. Cramer, J. T. Hupp and O. K. Farha, *Nat. Mater.*, 2015, **14**, 512.
15. A. M. Ploskonka and J. B. DeCoste, *J. Hazard. Mater.*, 2019, **In Press,** doi: 10.1016/j.jhazmat.2019.04.044.
16. D. L. Collins-Wildman, M. Kim, K. P. Sullivan, A. M. Plonka, A. I. Frenkel, D. G. Musaev and C. L. Hill, *ACS Catalysis*, 2018, **8**, 7068-7076.
17. M. C. de Koning, M. van Grol and T. Breijaert, *Inorg. Chem.*, 2017, **56**, 11804-11809.
18. A. X. Lu, M. McEntee, M. A. Browe, M. G. Hall, J. B. DeCoste and G. W. Peterson, *ACS Appl. Mater. Interfaces*, 2017, **9**, 13632-13636.
19. D. B. Dwyer, N. Dugan, N. Hoffman, D. J. Cooke, M. G. Hall, T. M. Tovar, W. E. Bernier, J. DeCoste, N. L. Pomerantz and W. E. Jones, *ACS Appl. Mater. Interfaces*, 2018, **10**, 34585-34591.
20. S. J. Garibay, I. Iordanov, T. Islamoglu, J. B. DeCoste and O. K. Farha, *CrystEngComm*, 2018, **20**, 7066-7070.
21. T. Islamoglu, M. A. Ortuño, E. Proussaloglou, A. J. Howarth, N. A. Vermeulen, A. Atilgan, A. M. Asiri, C. J. Cramer and O. K. Farha, *Angew. Chem. Int. Ed.*, 2018, **57**, 1949-1953.
22. G. W. Peterson, M. R. Destefano, S. J. Garibay, A. Ploskonka, M. McEntee, M. Hall, C. J. Karwacki, J. T. Hupp and O. K. Farha, *Chem. Eur. J.*, 2017, **23**, 15913-15916.
23. D. Bůžek, J. Demel and K. Lang, *Inorg. Chem.*, 2018, **57**, 14290-14297.
24. E. S. Hamborg and G. F. Versteeg, *J. Chem. Eng. Data*, 2009, **54**, 1318-1328.
25. P. Deria, W. Bury, I. Hod, C.-W. Kung, O. Karagiaridi, J. T. Hupp and O. K. Farha, *Inorg. Chem.*, 2015, **54**, 2185-2192.
26. S. T. Nguyen, J. T. Hupp, O. K. Farha and S. J. Garibay, *U.S. Patent No. 9,943,839.*, 2018.
27. H. Furukawa, F. Gándara, Y.-B. Zhang, J. Jiang, W. L. Queen, M. R. Hudson and O. M. Yaghi, *J. Am. Chem. Soc.*, 2014, **136**, 4369-4381.
28. T. Cottineau, M. Richard-Plouet, J.-Y. Mevellec and L. Brohan, *J. Phys. Chem. C*, 2011, **115**, 12269-12274.